Available online at www.sciencedirect.com
ScienceDirect
BioSystems 88 (2007) 323–333
BioSystems
www.elsevier.com/locate/biosystems

A Markovian engine for a biological energy transducer: The catalytic wheel

Tian Yow Tsong[a,b,*], Cheng-Hung Chang[c,d]

[a] *Institute of Physics, Academy of Sciences, Taipei 115, Taiwan*
[b] *National Chiao-Tung University and National Nanodevice Laboratory, Hsinchu 300, Taiwan*
[c] *Institute of Physics, National Chiao-Tung University, Hsinchu 300, Taiwan*
[d] *National Center for Theoretical Science, Hsinchu 300, Taiwan*

Received 11 January 2006; accepted 1 August 2006

Abstract

The molecular machines in biological cells are made of proteins, DNAs and other classes of molecules. The structures of these molecules are characteristically "soft", highly flexible, and yet their interactions with other molecules or ions are specific and selective. This chapter discusses a prevalent form, the catalytic wheel, or the energy transducer of cells, examines its mechanism of action, and extracts from it a set of simple but general rules for understanding the energetics of the biomolecular devices. These rules should also benefit design of manmade nanometer scale machines such as rotary motors or track-guided linear transporters. We will focus on an electric work that, by matching system dynamics and then enhancing the conformational fluctuation of one or several driver proteins, converts stochastic input of energy into rotation or locomotion of a receptor protein. The spatial (or barrier) and temporal symmetry breakings required for selected driver/receptor combinations are examined. This electric ratchet consists of a core engine that follows the Markovian dynamic, alleviates difficulties encountered in rigid mechanical model, and tailors to the soft-matter characteristics of the biomolecules.

PACS: 87.16.Nn; 82.39.Fk; 05.40.-a

Keywords: Biological motors; Enzyme; Ratchet; Catalytic wheel

1. Introduction

The Earth had seen a rapid emergence of small life forms roughly 4 billion years ago. These early life forms had adopted nanometer scale molecular devices to perform wide varieties of life activity and to encode information, perpetuate their presence, and seek their dominance. Surprisingly the molecules these different life forms adopted to build their bodies, genomes, or mechanisms of regulation, communication and energy transduction, have remained for the most parts unchanged from the original choices although relative prominences have shifted gradually. The RNAs based biological world by now has been replaced with a system with ever increasing sophistication and division of labors. Here DNAs, RNAs, proteins, lipids, carbohydrates and other types of molecules and ions interplay to form a kaleidoscopic yet highly organized and interdependent world of the living state. This chapter focuses on a class of biomolecular machines, the catalytic wheel (CW) that is made mainly of proteins and investigates their fundamental designs in the hope that the working principles behind these molecular machines may benefit

* Corresponding author.
E-mail addresses: tsongty@phys.sinica.edu.tw, tsong001@umn.edu (T.Y. Tsong), chchang@phys.cts.nthu.edu.tw (C.-H. Chang).

0303-2647/$ – see front matter © 2006 Elsevier Ireland Ltd. All rights reserved.
doi:10.1016/j.biosystems.2006.08.014

biomedical research and shine light on future development of manmade nanometer scale devices.

For the convenience of discussion biomolecular devices are classified according to their degree of sophistication in structure and function.

1.1. Channel and carrier proteins (Garrett and Grisham, 2002; Tinoco et al., 2002; Nicholls et al., 1992)

The simplest biomolecular devices already possess the ability to select ion, molecule or ligand for passage and transport. The molecular and ionic transports mediated by these simple devices are passive, namely, the reaction proceeds downhill of the chemical potential gradient. Myoglobin which carries oxygen to the muscle and K^+ channels that select K^+ for passage through cell membranes are examples.

1.2. Biocatalyst enzymes (Garrett and Grisham, 2002; Tinoco et al., 2002)

An enzyme is a rate enhancer of a biochemical reaction. It is effective only for a specific type of biochemical reaction hence it differs from an ordinary chemical catalyst such as platinum black in which substrate specificity if existing at all is weak. An enzyme achieves strong specificity by its 3D structure which interacts only with its substrates but not with other kinds of molecule. This specificity also enables an enzyme to be a much more effective rate enhancer. For example, orotidine monophosphate decarboxylase can speed up the rate of the decarboxylation by 3×10^{17}-fold. This means a reduction of the activation energy of the reaction (65 k_BT) by 39 k_BT. No chemical catalysts can achieve such catalytic power.

1.3. Energy transducer, the catalytic wheel (Tsong and Astumian, 1987; Tsong and Chang, 2003, 2005; Rozenbaum et al., 2004)

Since a catalyst recycles in each catalytic reaction, it may be regarded as a catalytic wheel. However, in this communication the CW means that the protein device is designed not only to speed up the rate of a biochemical reaction but also to convert energy from one form to another. In other words, it is a catalyst as well as an energy transducer. This type of devices is complex and usually consists of two or more different protein subunits. Examples are mitochondrial F_oF_1 ATPase and muscle myosin. The former is to synthesize ATP by the electrochemical potential energy of the mitochondrial membrane and the latter is to hydrolyze ATP to generate power stroke for the muscle contraction. Both are protein complexes composed of a dozen different protein subunits. A CW can harvest energy from its environment to support active, i.e. uphill transport of ions, molecules, or locomotion of particles, or to perform mechanical work.

2. Conformational flexibility of protein

As will be shown later for a CW to work as intended it must have at least two different conformational states (e.g. E^+ and E^-) (Tsong and Astumian, 1987; Tsong and Chang, 2003, 2005; Rozenbaum et al., 2004). In the physiological condition these conformations coexist and undergo dynamic fluctuation according to their energetic and kinetic attributes. The conformation (or structure in solution) of a protein can easily be changed by acids, ions, chemicals, temperature, pressure, electric field, etc. It may also be changed by interacting with substrate or ligand. In view of the current interest pertaining effect of thermal noise on protein function let us consider the thermally induced conformational change of an enzyme E in an aqueous solution:

$$E^+ \underset{k_{-,+}}{\overset{k_{+,-}}{\rightleftarrows}} E^-, \qquad K_{eq} = \frac{k_{+,-}}{k_{-,+}} \tag{1}$$

Here $k_{+,-}$ and $k_{-,+}$ denote, respectively, the forward and the backward rate constants and K_{eq} denotes the equilibrium constant of the conformational change. At a constant temperature K_{eq} is governed by the free energy difference between E^+ and E^- according to the relationship, $K_{eq} = \exp -[\Delta G^\circ/RT]$. For most proteins K_{eq} is also dependent on temperature by the van't Hoff equation (Tinoco et al., 2002; Tsong et al., 1970),

$$\left[\frac{\delta\ (\ln\ K_{eq})}{\delta\ T}\right]_P = \frac{-\Delta H^\circ}{T^2} \tag{2}$$

In a laboratory K_{eq} is determined by various experimental methods and the free energy of the reaction ΔG° is obtained. The enthalpy of the reaction ΔH° can be calculated with Eq. (2). If the reaction is more complex than the two-state reaction of Eq. (1), determination of ΔH° becomes less straightforward. In such a case microcalorimetry is employed to measure ΔH° directly. For a typical small globular protein, e.g. staphylococcal nuclease (149 amino acids) ΔH° of unfolding is approximately 100 kcal mol^{-1} (159 k_BT molecule^{-1}), and yet ΔG° of the same reaction is a mere 5 kcal mol^{-1} (8 k_BT molecule^{-1}) (Tsong et al., 1970; Tsong and Su, 1999). The heat capacity change ΔC_P due to the thermal transition is 2.2 kcal mol^{-1} K^{-1} (3.5 k_B molecule^{-1}) (Tsong et al., 1970). The entropy of the E^+ to

E^- transition is thus, $\Delta S^\circ = [\Delta H^\circ - \Delta G^\circ]/T = -95\,\text{kcal mol}^{-1}\,\text{K}^{-1} = -150\,k_B\,\text{molecule}^{-1}$.

These thermodynamic quantities reveal one interesting fact; although the enthalpy of the protein structure is nearly $-160\,k_BT$, its stability or ΔG° is a small fraction of the ΔH°, $-8\,k_BT$. This value is equivalent to the energy of a few hydrogen bonds. In a protein of this size, there are hundreds of hydrogen bonds, salt-bridges, and hydrophobic contacts within its 3D structure. Yet its net conformational energy, or stability, is equivalent to only a few hydrogen bonds. This extraordinary property of protein is known as the enthalpy/entropy compensation, and is attributed to the protein interaction with the solvent water (Tinoco et al., 2002; Tsong et al., 1970; Tsong and Su, 1999). An unfolded protein tends to expose its hydrophobic residues to solvent water and this causes the ordering of the water molecules surrounding the hydrophobic moieties resulting in negative entropy change overall. Because of the marginal stability and a large ΔH° value of a CW, the range of temperature it can function is very narrow indeed, usually between 20° and 40°. Beyond this temperature range the CW loses its ability to undergo functionally important conformational changes. Manmade machines have a much broader tolerance for temperature variations. The energy difference between the functional forms of a CW, E^+ and E^- is likely smaller than the value $8\,k_BT$ which is for the folding–unfolding of the 3D structure. Notice that the ambient thermal noise is of the order $1.5\,k_BT$. The marginal stability of protein structure is thus highly susceptible to perturbation by the thermal noise.

Another property of protein deems important to the study of the CW concerns the molecular dynamics, or the flexibility of the structure. In the protein structure there are many degrees of freedom and their modes of motion span broad ranges in time (Garrett and Grisham, 2002; Tinoco et al., 2002). For examples, the vibration and rotation of chemical bond occur in the femtosecond to the picosecond time ranges, the flip-flop of organic rings within protein structure in the nanosecond to the millisecond time ranges, electron transport among prosthetic groups in the femtosecond to the picosecond time ranges, local chain motion in the nanosecond to the millisecond time ranges, folding–unfolding transition in the microsecond to the second time ranges, subunit association and dissociation, and aggregation and disaggregation in the nanosecond to the minute time ranges. And there are other slow modes of motion ranging in days that are measurable by the hydrogen exchange technique. The range of dynamics spans at least 17 decades in time.

3. A two-state engine fueled by stochastic input of energy

Are these structural fluctuations and dynamics relevant to the function of the CW and if so, how? Today the single molecule technology can monitor or measure conformational fluctuations of a protein or a CW directly and in real time (Vale et al., 1996; Yasuda et al., 1998, 2001; Xie and Lu, 1998). All the thermodynamic and dynamic information is contained in these data. If the conformational change is triggered by a stochastic driving force, the switching dynamics of Eq. (1) is Markovian (Tsong and Astumian, 1987; Tsong and Chang, 2005; Makhnovskii et al., 2004). Later in this chapter it will be shown that in a CW some chemical processes may be slow and not totally stochastic. However, if the conformational change of $E^\pm$ is rapid compared to other chemical processes and the mean frequency of the switching dynamic, it should manifest a Markovian behavior (Makhnovskii et al., 2004; Markin and Tsong, 1991b, 1993). This will form the basis of our formulation of a Brownian ratchet mechanism for the CW.

Fig 1 illustrates the two conformational states of an ion transporter (E^+ and E^-). Their interaction profiles, or the activation barriers with an ion ($U^+(x)$ and $U^-(x)$) for the (+) and (−) reservoirs, respectively, are also indicated. By the shape of the $U^\pm(x)$ in this case, E^+ tends to capture an ion from the (+) reservoir and E^- tends to release the captured ion into the (−) reservoir (Tsong and Chang, 2003, 2005; Rozenbaum et al., 2004; Markin et al., 1992). The membrane is not permeable to the ion and ion transport across the membrane must rely on the transporter to mediate. This in turn requires the transporter to undergo reversible conformational changes between E^+ and E^-. In other words, an ion will have to surf along the $U^\pm(x)$ surface to move forward or backward. The E^+ to E^- transition, and vice versa, may be triggered by the thermal noise, as mentioned above, or by hydrolysis of ATP or by an applied pressure, or electric field (Tsong and Astumian, 1987, 1986; Teissie et al., 1981; Serpersu and Tsong, 1983; Tsong, 1990). Notice that the ion in the (+)-hand side is distinguishable from the ion in the (−)-hand side by virtue of their difference in the chemical potential ($\mu_+ \neq \mu_-$). The difference in the chemical potential ($\Delta\mu_{+,-} = \mu_- - \mu_+$), if positive, will be the work to overcome for moving an ion rightward.

Let us define $U^\pm(x)$ by the activation barriers v and V, and a load by F as shown in Fig. 2 (Rozenbaum et al., 2004; Tsong and Chang, 2005; Makhnovskii et al., 2004). Here the potential profiles shown in Fig. 1 are linked alternately to form an 1D potential energy surface

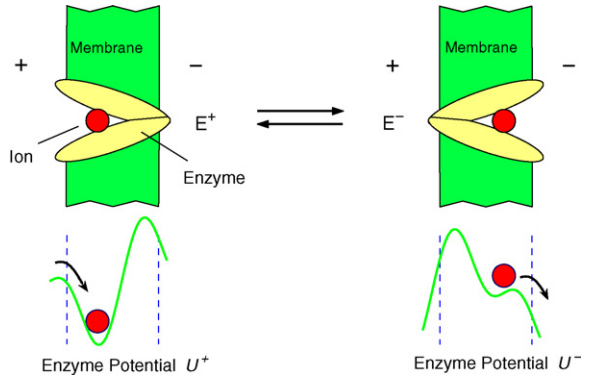

Fig. 1. Conformational switching of a membrane transporter. An ion transporter is used as an example. When it is in the E^+ form its ion binding site faces the (+) reservoir. The transporter is assumed to have a high affinity for the ion as indicated by its deep-well potential. When E^+ is converted to E^- the ion binding site now faces the (−) reservoir. Here the interaction potential favors the release of ions from the protein. Any cyclic switching, or ratcheting between E^+ and E^- will result in transport of ions rightward.

for the ion to surf along the reaction coordinate x. From the upper curve (U^-) we notice that the potential profile so constructed has an undulating feature with a periodicity of L. Likewise the U^+ has a shape identical to U^- but is shifted rightward by one half of the period, $L/2$, i.e. $U^+(x) = U^-(x + L/2)$. The parameters that specify U^+ and U^-, namely v and V are related to chemical rate constants of ion binding and dissociation in E^+ and E^- states in the absence of the applied force as discussed in details elsewhere. The difference of the chemical potential $\Delta\mu$ is represented by the work FL of a force F done along a period L.

The switching of the U^+ to U^- transition and vice versa, by an applied force modulates these barriers and actuates the transporter to pump ions rightward (Rozenbaum et al., 2004; Tsong and Chang, 2005; Makhnovskii et al., 2004). The effect is graphically illustrated in Fig. 2. In U^- when an ion (or a particle) is located at the valley 2 it tends to move rightward to valley 1. At this instant, U^- switches to U^+ and the particle at valley 1 is relocated to valley 2 and it continues to move rightward because of lesser barrier height v than the leftward barrier V. In other words, any conformational fluctuation between E^+ and E^- will result in the rightward transport of ions and this will continue and stop when the chemical potential difference equals $V - v = FL \equiv \Delta\mu$.

4. Catalytic wheel and the energy coupling

There are many ways to drive a Markovian engine of Fig. 1. However if the energy absorbed by the molecule E is not channeled to usage it will dissipate into the environment as heat in picoseconds. A CW is to extract energy to perform chemical or physical work, and as such some means of energy coupling must be built into

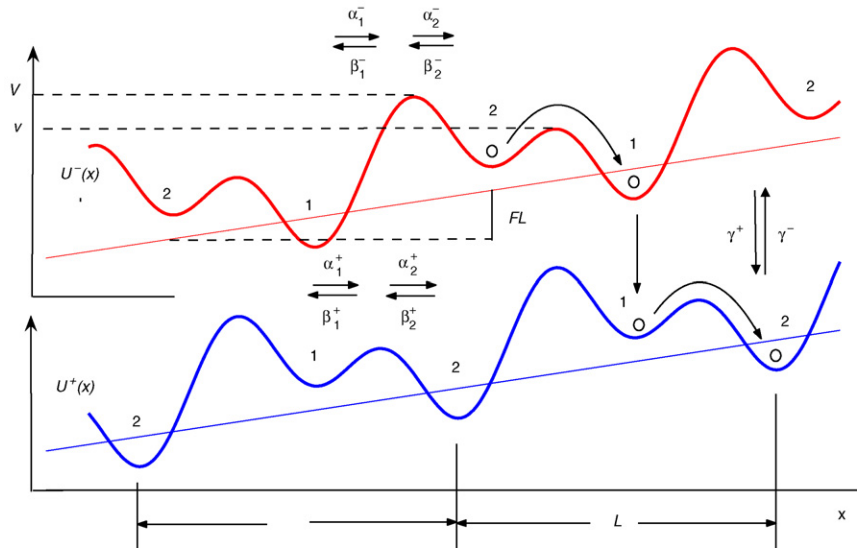

Fig. 2. The two interaction potentials shown in Fig. 1 are linked and repeated to form a potential profile with a periodicity of L. In the upper profile $U^-(x)$ a particle tends to move from well 2 to 1. An external driving force is then applied to switch the state of E. This switching is equivalent to shifting the $U^-(x)$ to $U^+(x)$ rightward by $L/2$. The particle initially on the well 1 now moves to well 2. $U^+(x)$ is then switching by $L/2$ reaching $U^-(x + L/2)$. And the particle moves rightward again. The particle moves rightward on repeated switching of states. This conformational fluctuation system is equivalent to a two-state Brownian ratchet. Here the work for the ratchet is expressed as Fx. For details see (Rozenbaum et al., 2004).

its mechanism (Tsong and Astumian, 1987, 1986; Tsong, 1990). Let us consider the four-state model shown in Fig. 3. Here to the two-state Markovian engine of Fig. 1 is added a Michaelis–Menten enzyme (MME) mechanism (Rozenbaum et al., 2004; Tsong and Chang, 2005),

$$E^+ + S \leftrightarrow E^+S \leftrightarrow E^-P \overset{k_{cat}}{\rightarrow} E^- + P \tag{3}$$

in which, S and P are, respectively, the substrate and the product. The MME model simply states that for an enzyme to catalyze a reaction it must associate with its substrate, S. The S is then converted to the product P while still on enzyme surface. This S to P conversion inevitably changes the conformational state of the enzyme and that greatly weakens enzyme affinity for P. Subsequently, P dissociates and the enzyme (E^-) returns to its initial state (E^+) before it can capture a substrate again. The reaction is cyclic and during each cycle the enzyme turns over. For example, if S is ATP, P will be ADP and P_i, and if S is a cation in the (+) reservoir P will be the same ion in the (−) reservoir. Enzyme turn-over rate is proportional to k_{cat} in the MME model.

The four-state CW in Fig. 3 has been studied in great details in our laboratory. Indeed it is just a four-state cyclic chemical reaction to each step rate coefficient $k_{i,j}$ can be assigned and the dynamics of the CW can be computed by the standard chemical kinetic method, i.e. by solving the Master equation (Tsong and Astumian, 1987; Rozenbaum et al., 2004; Makhnovskii et al., 2004). Here all the rate constants involving E^+ and E^- become time-dependent once an external force, which is time-dependent, is applied to enforce the conformational transitions between E^+ and E^- and between E^+S and E^-P (Tsong and Astumian, 1987; Markin and Tsong, 1991b, 1993) (see also Eq. (6)). We now turn to the discussion of an electroconformational coupling (ECC) model based on the CW mechanism (Tsong and Astumian, 1987, 1986; Tsong, 1990).

A cell maintains a constant transmembrane electric potential of the order of −100 mV (Nicholls et al., 1992). This electric potential may be modulated by transport of electron on membrane surface amid electron carrier groups such as heme, flavin mononucleotide (FMN), etc. Passage of ions through a channel protein may also modulate local membrane electric potential. Fluctuation of transmembrane potential in the 100 mV range is commonplace (Nicholls et al., 1992; Tsong and Astumian, 1987; Tsong, 1990). These processes are stochastic and can trigger electroconformational change of a membrane integral protein according to the

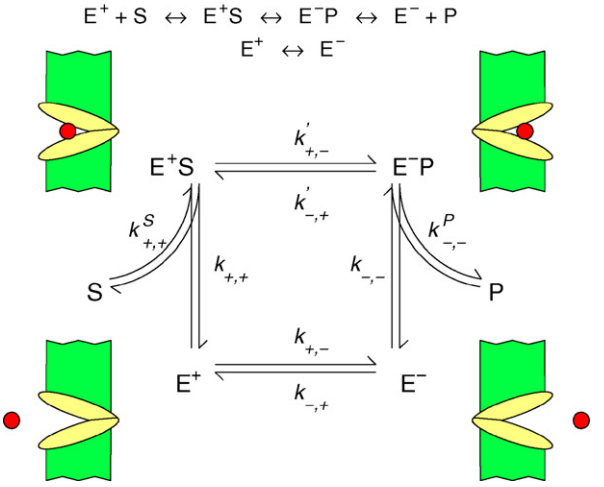

Fig. 3. A catalytic wheel (CW) for energy coupling. The conformational ratchet model of Fig. 1 is coupled to a Michaelis–Menten enzyme (MME) to construct a CW. The cartoon for the cyclic reactions in the lower part depicts the identical chemical events of the two chemical equations (MME) shown on the upper part. The E^+ and E^- transition is enforced by an external force, e.g. by thermal fluctuation, applied electric field, or ATP hydrolysis. The absorbed energy is coupled to driving an active transport or an uphill biochemical reaction.

relationship,

$$\left[\frac{\delta\,(\ln K_{eq})}{\delta\,\boldsymbol{e}_m(t)}\right]_{P,V,T} = \frac{\Delta \boldsymbol{M}}{RT}. \tag{4}$$

Here $\Delta \boldsymbol{M} = \boldsymbol{M}^- - \boldsymbol{M}^+$ with the molar electric moment $\boldsymbol{M}^\pm$ of $E^\pm$,

$$\boldsymbol{M}^\pm = N_{Av} \sum_i [(z_i^\pm \boldsymbol{d}_i^\pm + \boldsymbol{\mu}_i^\pm) + \alpha^\pm \boldsymbol{e}_m(t)], \tag{5}$$

where N_{Av}, $z_i^\pm$, $\boldsymbol{d}_i^\pm$, $\boldsymbol{\mu}_i^\pm$, and $\alpha^\pm$ are, respectively, the Avogadro number, the net charge, the distance of the *i*th group, and the permanent dipole moment (peptide backbone, etc.), and the electric susceptibility of the structure. Notice that the transmembrane effective electric field intensity, $\boldsymbol{e}_m(t)$ is a time dependent quantity. Both $\boldsymbol{e}_m(t)$ and $\Delta \boldsymbol{M}$ are vector quantities. The dot product $\Delta \boldsymbol{M} \cdot \boldsymbol{e}_m(t)$ is a scalar quantity and equivalent to free energy change due to the electrostatic interaction of $E^\pm$ with the $\boldsymbol{e}_m(t)$. Thus the free energy of the interaction is a time variable and so is the K_{eq}. The rates of the electric filed induced transitions of $E^\pm$ and of $E^\pm L^\pm$ will also depend on the applied field (Tsong and Astumian, 1987, 1986; Tsong, 1990):

$$k(t) = k^0 \exp\left(\boldsymbol{e}_m(t) \cdot \frac{\Delta \boldsymbol{M}}{RT}\right). \tag{6}$$

Experiment in our laboratory has employed electric field of different waveforms to trigger switching of $U^\pm(x)$

for the Na,K-ATPase of human erythrocyte membrane (Serpersu and Tsong, 1983, 1984; Liu et al., 1990; Xie et al., 1994, 1997). Two of the stochastic wave trains are shown in Fig. 4. The first dichotic waveform is a flat top random telegraph function with a mean pulse width t^*, $t = t^* \ln R$. Here R is a random number between 0 and 1 and the pulse width t has a Poisson distribution centered at t^*. There are only two discrete values for the applied electric field, $+\Delta$ or $-\Delta$. The two values are chosen to generate transmembrane effective electric potential of +25 and −25 mV, respectively. The thickness of the cell membrane is approximately 5 nm and the effective electric field experienced by Na,K-ATPase is, thus, $\pm 5 \times 10^6\ \mathrm{V\,m^{-1}}$. This field strength was estimated to be in the right order of magnitude to induce inward pumping of K^+ and outward pumping of Na^+, both up a concentration gradient of approximately 10.

The second wave train shown in Fig. 4 has a Gaussian distribution of the amplitude, $G(\Delta) = [\sigma\sqrt{\pi}]^{-1} \exp[(\Delta - \Delta^*)^2/2\sigma^2]$, where Δ^* and σ are, respectively, the mean amplitude and the standard deviation of the amplitude. Both wave trains activate the Na^+- and the K^+-pumping modes of Na,K-ATPase (Xie et al., 1994, 1997).

Notice that if E^+ to E^- transition has a non-zero ΔH° a temperature fluctuation will drive conformational fluctuation according to Eq. (2). Can an ion transport be induced by the ambient thermal noise (equilibrium noise) in the absence of an applied force? Our

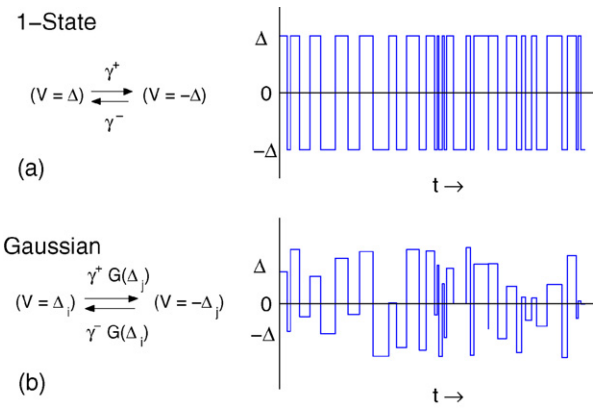

Fig. 4. Stochastic switching of states of Fig. 1. The upper curve (a) represents a stochastic switching of electric field between $+\Delta$ and $-\Delta$ according to the random telegraph function. The electric pulses enforce the conformational fluctuation of Fig. 1. Only one discrete type of transition is allowed. In the lower curve the $\Delta^{\pm}$ has a Gaussian distribution with a standard deviation σ. The conformational switching in this case may be partial. See Section 6 for details. Note that the symbols $G(\Delta_i)$ and $G(\Delta_j)$ above and below the arrows in (b) mean that the amplitudes Δ_i and Δ_j follow a Gaussian distribution.

treatment of the four-state transport model of Fig. 3 has shown that this cannot occur if detailed balancing and microscopic reversibility are strictly obeyed (Tsong and Astumian, 1987, 1986; Tsong, 1990; Serpersu and Tsong, 1984). In other words, an equilibrium thermal noise cannot fuel a CW. Only an off-equilibrium periodic or stochastic input of energy can. Furthermore, most organisms are homeothermal and their body temperatures are constant. Quite often a local temperature gradient in nanometer scale dissipates rapidly (for more complex cases of slow dissipations, see Weaver et al., 1999). Thus, to use an externally generated off-equilibrium thermal noise to drive slower, functionally relevant conformational transition of E can only be done in some special chemical environment, e.g. in a gel-like environment. Thermal relaxation in gel-like environment is slow. Small conformational fluctuation of a protein or a change in the hydration layers surrounding its structure does have rapid relaxation time in the picosecond time range. If these fast relaxation processes are functionally relevant, an off-equilibrium thermal noise may drive a CW via the Brownian ratchet mechanism.

The transduction of a sound wave poses a familiar case for the CW. An acoustic wave is a form of pressure oscillation and involves in hearing transduction of the hair cells inside the ear work. If the transition of E has a non-zero molar volume change ΔV° for the E^+ and E^- transition, a fluctuation in pressure will drive a conformational fluctuation according to the thermodynamic relation, $[\delta(\ln K_{eq})/\delta P]_T = -\Delta V^\circ/RT$. A pressure sensitive ion pump has been discussed in relation to the transduction of the sound wave (Markin and Tsong, 1991c).

We should emphasize that a CW can function as a track-guided 1D transporter as well. For a myosin to move along a F-actin cable the Barrier Surfing Model (Tsong and Chang, 2003, 2005) considers a myosin head S1 to have two conformational states $S1^+$ and $S1^-$ depending on its interaction with ATP, ADP, or lack of it. If the interactions of $S1^+$ and $S1^-$ with F-actin are asymmetric as U^+ and U^- in Fig. 1, any ratchet effect enforced on S1 will move the S1 along the 1D barrier profiles shown in Fig. 2. S1 will move rightward whenever a transition of the conformational state of S1 is induced by an ATP hydrolysis or by an applied force. The two head situation in myosin and kinesin systems requires extra attention. However, construction of a workable model for a two head motor is a challenge of the detail not of the fundamental principle. Section 6 will deal partially with this issue.

5. Matching two interacting dynamics

For a CW to work a protein must be able to interact with an applied force (Tsong and Astumian, 1987, 1986; Tsong, 1990). However, the efficiency of the energy coupling is dependent on the two interacting dynamics of the system: first, the thermodynamics and the kinetics that specify the chemical reactions of the CW in the absence of the applied force and second, the dynamics of the applied force. If the applied force is electrostatic, Eqs. (4)–(6) apply. An oscillating or fluctuating electric field will interact with the CW and the electric energy will be effectively converted to the chemical bond energy of ATP or the chemical potential energy of an ion. Analysis of the four-state CW of Fig. 3 has clarified many important properties of the system. Readers are referred to journal articles for details (Tsong and Astumian, 1987, 1986; Tsong and Chang, 2003; Rozenbaum et al., 2004; Makhnovskii et al., 2004; Markin and Tsong, 1991b,c, 1993; Markin et al., 1992; Teissie et al., 1981; Serpersu and Tsong, 1983, 1984; Tsong, 1990; Liu et al., 1990; Xie et al., 1994, 1997). Some features are outlined in the following.

5.1. Optimal amplitude, frequency, and ligand concentration for energy coupling (Tsong and Astumian, 1987, 1986; Markin and Tsong, 1991b; Serpersu and Tsong, 1983, 1984; Tsong, 1990; Liu et al., 1990; Xie et al., 1994, 1997)

Under-drive or over-drive of the conformational transition obviously reduces the efficiency of a CW. The contribution of the electric susceptibility term $\alpha^{+}\boldsymbol{e}_{\mathrm{m}}(t)$ to the interaction energy, $\Delta\boldsymbol{M}\cdot\boldsymbol{e}_{\mathrm{m}}(t)$ is always positive, since it is quadratic in $\boldsymbol{e}_{\mathrm{m}}$ (see Eq. (5)). If this term becomes a dominating term, the $\boldsymbol{e}_{\mathrm{m}}(t)$ will lock the E into one conformation and prevent E to turnover (Tsong and Astumian, 1986; Tsong, 1990). This will reduce the efficiency of the energy transduction. The amplitude of the energy input, or of the applied field, has an optimal value. The optimal frequency is related to enzyme turnover. When the frequency of the applied force matches the turnover rate (e.g. k_{cat}) the energy transduction is effective. In the experiment with Na,K-ATPase the optimal amplitude for both Na^{+} and K^{+} pumps is $\pm 5\times 10^{6}\,\mathrm{V\,m^{-1}}$ as mentioned above. The ECC analysis of the CW of Fig. 3 verifies these experimental observations. The optimal frequency for K^{+}-pump is 1.0 kHz. However, the optimal frequency for the Na^{+} pump is 1.0 MHz. Thus, the Na^{+} and the K^{+} pumps may be uncoupled by a frequency tuning, contrary to the biochemical studies which show that the two pumps are coupled under the physiological condition. Our interpretation is that the coupling of the two pumps requires phosphorylation of the Na,K-ATPase. In the electric activation experiment, [ATP] and the temperature are kept low. No phosphorylation is likely to take place (Serpersu and Tsong, 1984; Liu et al., 1990; Xie et al., 1994, 1997).

5.2. Kinetics of energy coupling (Rozenbaum et al., 2004, 2005; Makhnovskii et al., 2004; Markin and Tsong, 1991b,c, 1993; Markin et al., 1992; Serpersu and Tsong, 1983; Tsong and Astumian, 1986; Tsong, 1990; Serpersu and Tsong, 1984; Liu et al., 1990; Xie et al., 1994, 1997)

The above optimum system interaction is achieved when three conditions are met. Firstly, referring to Fig. 2 if $V \gg v$ the backward transport is effectively prevented. The second one is the steepness, or the narrowness in width, of the barrier V. The third condition to achieve a high efficiency according to model analysis is to maintain the inequality, (rates of conformational changes between E^{+} and E^{-} and between $E^{+}S$ and $E^{-}P$) $\gg$ (frequency of applied force) $\gg$ (rates of ligand association and dissociation) (Markin and Tsong, 1991a; Markin et al., 1990). Under these conditions the maximal efficiency of the CW can be close to unity.

5.3. Rectification and pumping (Markin and Tsong, 1993, 1991a)

Oscillation of an electric field may drive transport of ions by rectification. One astonishing finding of our analysis by the Brownian ratchet mechanism is that the ion rectification mechanism cannot achieve more than 8.7% of efficiency (Markin and Tsong, 1991a). Various mechanisms involving mixing of the conformational coupling and the ion rectification effects have been examined in detail elsewhere (Markin and Tsong, 1993, 1991a).

5.4. Reversal of particle movement (Markin and Tsong, 1993, 1991a; Markin et al., 1990)

A heavy load can cause the reversal of a particle movement. Referring to Figs. 1 and 2, the particle in the valley 1 under the potential $U^{+}(x)$ of Fig. 2 must climb the right barrier v or the left barrier V before it reaches its next right and left valleys. When $v = V$ the net transport flux vanishes to zero. And when $v > V$, the asymmetry direction is reversed. In Fig. 2 each switching between U^{+} and U^{-} will result in the leftward movement of the particles.

In the case of enzyme catalysis P is now converted to S. The reverse energy transduction is also highly efficient for the conformational coupling model with the Brownian ratchet mechanism (Markin and Tsong, 1993, 1991a; Markin et al., 1990), similar to F_1ATPase. This ATPase is known to synthesize ATP by the applied mechanical force that turns the γ-subunit in the direction opposite to that of the ATP hydrolysis (Itoh et al., 2004). ATP synthesis by the applied electric pulses has also been demonstrated for the submitochondrial particles (Teissie et al., 1981).

6. A dipole ratchet model (DRM)

The basic working principle of a CW is its cyclic conformational changes. In previous sections we have shown a CW may induce a chemical catalysis, transport an ion across a membrane, or move a particle along a track. This section will give an example to illustrate how CWs can rotate a protein complex in a DRM. As an example a DRM designed for a rotary motor is shown in Fig. 5. In the figure the three driver proteins are located in a plane with equal angular separation of 120° to each other. For simplicity, the three drivers are assumed to be identical and each has an electric dipole of the same strength. Each driver has a low energy state with orientation w_1 and a high energy state with w_2. If some energy pulse is supplied to the driver, it may change from w_1 to w_2 and stay at the high energy state w_2 for a while. After this energy dissipates away, the driver comes back to w_1 again. The supplied energy needs not be electrical like that in Ref. (Teissie et al., 1981). It may be mechanical or in the case of biological motors chemical, for example, proton electrochemical potential energy, or the hydrolysis of ATP (Chang and Tsong, 2005). At the center of these three drivers is anchored a receiver protein rotor with a dipole in its structure. The positioning and the orientation of the receiver dipole are adjustable within the confine of the axial center. We asked the question if the three driver proteins (CWs) are three independent engines, what would happen if they are driven by stochastic energy pulses. What type of a motion in the receiver protein can the back-and-forth angular fluctuations of the three drivers generate? And what are the necessary conditions for the DRM to function as a rotary motor? Note that 'fluctuation' here stands for the switching of conformations by a stochastic driving force, for example, an electric field, an acoustic field, or a chemical potential. It is to be distinguished from the equilibrium thermal fluctuation which has a magnitude of kT. The applied force-induced fluctuation of a CW is mentioned through out the text. The evolution of the rotor orientation θ is described by the

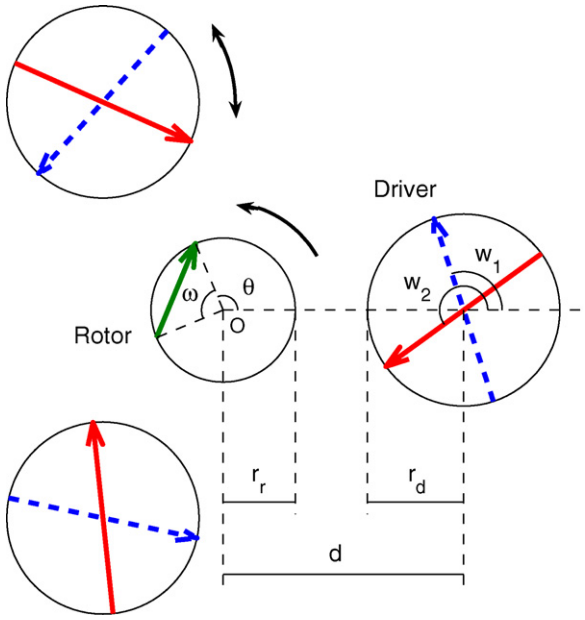

Fig. 5. A dipole ratchet with three drivers. Each driver has two conformational states with orientations w_1 and w_2.

equation,

$$J\ddot{\theta} + \Gamma\dot{\theta} + \frac{\mathrm{d}U(\theta)}{\mathrm{d}\theta} = 0, \tag{7}$$

where J is the moment of inertia of the rotor, Γ, a damping constant, and $U(\theta)$, an orientation dependent Coulomb potential,

$$U(\theta) = \sum_{a,b} \frac{Kq_a^{\mathrm{R}}q_b^{\mathrm{D}}}{|R_a^{\mathrm{R}}(\theta) - R_b^{\mathrm{D}}|}, \tag{8}$$

where K is the Coulomb's constant, q_a^{R} with $a \in \{\pm 1\}$ denotes the positive and negative effective charges on the two ends of the rotor dipole and the vector $R_a^{\mathrm{R}}(\theta)$ stands for their locations. Similarly, q_b^{D} with $b \in \{\pm n\}$, where $n = 1, \ldots, N$ ($N = 3$ for the example in Fig. 5), represents the positive and negative charges on the two ends of the nth driver dipole and the vector $R_b^{\mathrm{D}}(\theta)$ stands for their locations. On the complex plane, the vectors $R_a^{\mathrm{R}}(\theta)$ and R_b^{D} can be denoted by the complex numbers $P_l^{\mathrm{R}}(\theta) = r_{\mathrm{r}}\mathrm{e}^{\mathrm{i}[\theta+l\omega]}$ and $P_{jkl}^{\mathrm{D}} = d\mathrm{e}^{\mathrm{i}[2\pi(j-1)/N]} + r_{\mathrm{d}}\mathrm{e}^{\mathrm{i}[2\pi(j-1)/N+l\pi+w_k]}$, where r_{r} (r_{d}) is the radius of the rotor (driver) and d denotes the distance between the rotor center and the driver center (Fig. 5). The indices $j \in \{1, 2, \ldots, N\}$, $k \in \{1, 2\}$, and $l \in \{0, 1\}$ stand for the jth driver, its two conformational states, and their positive and negative charges, respectively. As an example, the parameters are selected as follows: $J = 0.01$, $\Gamma = 0.005$, $K = q_a^{\mathrm{R}} = q_b^{\mathrm{D}} = 1$, $r_{\mathrm{r}} = 2$, $r_{\mathrm{d}} = 6$, $d = 10$, $\omega = \pi/10$, $w_1 = \pi/2$, and $w_2 = \pi$.

A surprise finding of this DRM is that the back-and-forth conformational fluctuation of the three uncorrelated drivers can propel unidirectional rotation of the central receiver if certain asymmetries are met. Note that uncorrelation here and later means the motion of a driver does not depend on the motion of the other drivers.

6.1. Spatial symmetry breaking

For simplicity let us consider a DRM with $N = 2$ drivers and each driver has two conformations, say, A and B. Originally, these drivers are supposed to stay at certain conformations (A, B), that is, the first driver at A state and the second driver at B state. Under this arrangement the rotor dipole with orientation θ feels a potential $U_1(\theta)$ in Fig. 6 (a). When the first driver changes its conformation from A to B and the second from B to A, the system has a new driver conformation (B, A) and gives another potential U_2 to the rotor. While these two drivers stochastically vibrates, the system randomly switches between $2^N = 4$ different potentials. Among them, the two significant potentials U_1 and U_2 are asymmetric with the same biased direction. Therefore, when the rotor dipole is exposed to these potentials, it is more likely to be driven unidirectionally in the biased direction of these potentials, i.e., rightward in the example of Fig. 6. In Fig. 5 the positioning of the dipole in the receiver protein is of crucial importance, because it determines the potential asymmetry and the rotation direction. If the receiver dipole is put on the center of the rotor, the DRM does not have any spatial asymmetry and no unidirectional rotation will occur. This spatial symmetry breaking induced rotational works for all DRM systems with driver number larger than one, e.g., Fig. 6 (a)–(c). For DRM with one driver, the only two potentials have opposite biased directions, e.g., U_1 and U_2 in Fig. 6 (d). The rotor dipole to be moved in opposite directions is equally likely. Therefore, DRM of one driver cannot perform unidirectional rotation by spatial symmetry breaking. But it still can happen if the temporal symmetry of the system is broken (Chang and Tsong, 2005).

A dipole ratchet has already been found to play a significant role in the ion pumping by Na,K-ATPase (Serpersu and Tsong, 1983, 1984; Liu et al., 1990; Xie et al., 1994, 1997). In this respect it is tempting for us to examine if the 3-drivers 1-receiver case may mimic the behavior of the F_oF_1ATPase (Yasuda et al., 1998, 2001). So far we have treated three uncorrelated drivers, however this assumption needs not be binding. With biological machines in transit for billions of year they may have developed more elaborate regulation mechanism with which to improve the efficiency or to facilitate control. The DRM of Fig. 5 is tested for the uncorrelated fluctuation as well as for the sequential activation of the three drivers. The result is compared in Fig. 7. It appears

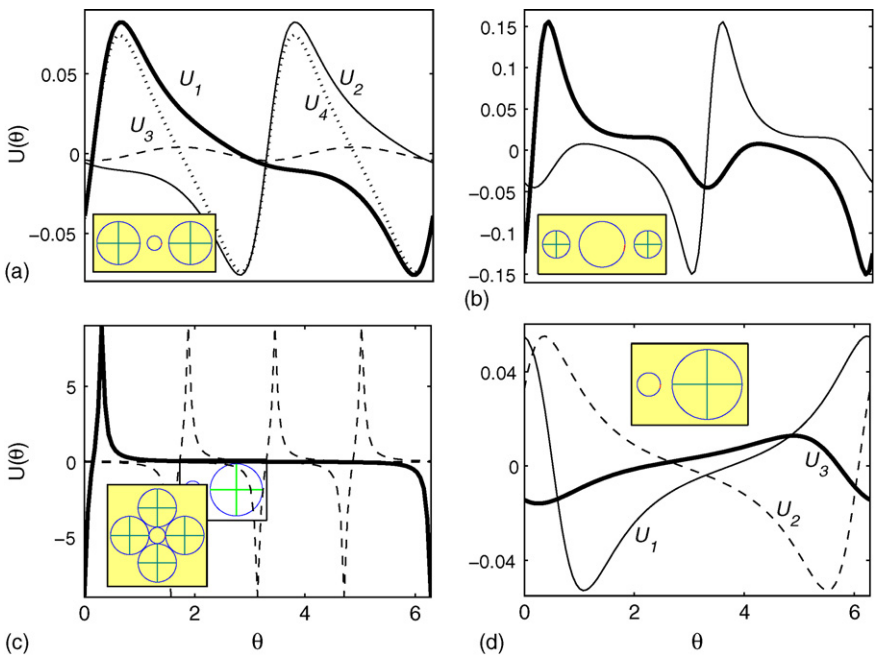

Fig. 6. Ratchet potentials for different rotor and driver configurations in the inset with $d = 10$ and $(N, \rho_r, \rho_e) = (2, 0.2, 0.2)$, $(2, 0.5, 0.2)$, $(4, 1 - (\sqrt{2}/2), 0.01)$, and $(1, 0.2, 0.2)$ in (a), (b), (c), and (d), respectively, where $\rho_r = r_r/d$ and $\rho_e = (d - r_r - r_d)/d$.

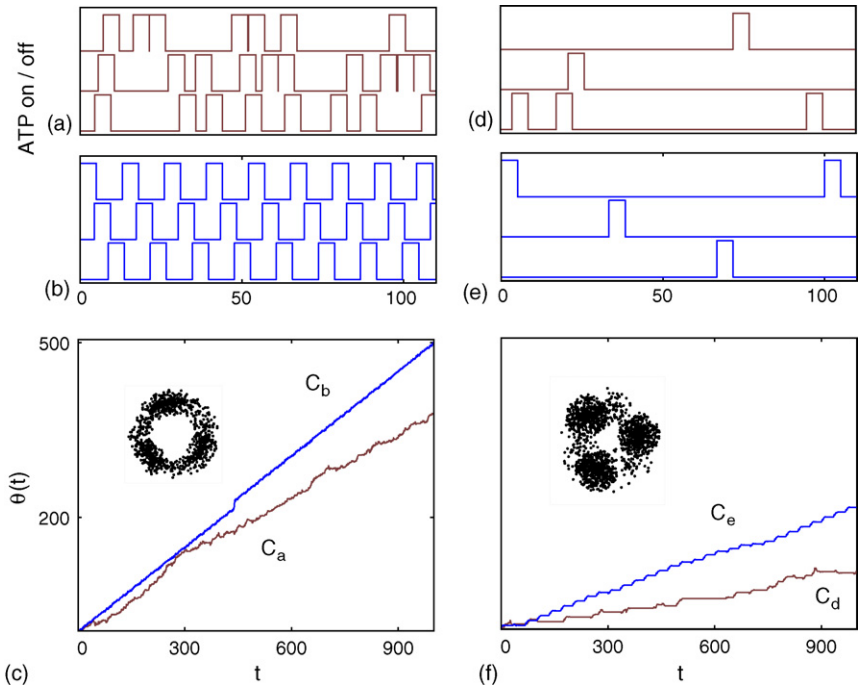

Fig. 7. After an ATP is supplied to a driver, it is changed to the high energy state and stays there for a period of $\tau = 5$ time units. Thereafter it comes back to the low energy state again. (a) and (d) The state sequences of the three drivers are under stochastic energy pulses. (b and e) The state sequences are under periodic ATP pulses. (c and f) The corresponding rotor angles $\theta(t)$ and the spatial locations of the bead (Chang and Tsong, 2005). (a and b) [(d) and (e)] correspond to high [low] ATP concentration.

that for the sequential activation the speed of rotation is higher than the uncorrelated case. We also found that in fact the 3-driver 1-receiver configuration of Fig. 5 is an optimal arrangement although systematic study remains to be done.

According to the Chemiosmotic Hypothesis, ATP synthesis in mitochondria is by the transduction of electrochemical potential energy through the action of F_oF_1ATPase. When the transmembrane proton concentration gradient is sufficiently large, the proton flux through the F_o subunit drives the central γ axis to rotate. Since γ is not centrally symmetric, its rotation applies power strokes to the three surrounding β subunits in a clockwise time sequence (Garrett and Grisham, 2002; Yasuda et al., 1998, 2001; Wang and Oster, 1998). These sequential conformational changes of the βs induce ATP synthesis. However, if the transmembrane proton gradient is low and the ATP concentration is high, ATP can instead hydrolyze and fuel βs to drive the rotation of γ in the opposite direction. While the ATP bombardment on each β is stochastic, docking and hydrolysis of ATP on βs are found to follow a counter-clockwise time sequence, indicating a structure correlation between these three separated β subunits. Interestingly, as shown in Fig. 7(c and f), although such correlation is not a necessary condition for a unidirectional rotation in the DRM, the efficiency from a correlated driving is better than a correlated driving. Cells seem to have selected a more complex and optimal mechanism for their ATP syntheses.

The DRM and F_oF_1ATPase share two common features. First, the asymmetric structure of the γ axis in F_oF_1ATPase provides sequential strokes to different βs (Garrett and Grisham, 2002). This asymmetric geometry suggests an asymmetric dipole on γ, which has been indicated in the experiment of Ref. (Teissie et al., 1981). This asymmetric dipole is also crucial for a unidirectional rotation in the DRM. Second, the driver and rotor configuration of the optimal rotation efficiency in the DRM is $N = 3$ which is the same as the numbers of β and γs in F_oF_1ATPase. The simplicity of and similarity in function of the uncorrelated DRM to the F_oF_1ATPase seem to suggest that some primitive molecular motors resembling the present model might exist during the early stage of the biological evolution.

References

Chang, C.H., Tsong, T.Y., 2005. Dipole ratchet for rotary molecular motors. Phys. Rev. E 72, 051901.

Garrett, R.H., Grisham, C.M., 2002. Principle of Biochemistry, With a Human Focus. Harcourt College Publishers, New York.

Itoh, H., Takahashi, A., Adachi, K., Noji, H., Yasuda, R., Yoshida, M., Kinosita Jr., K., 2004. Mechanically driven ATP synthesis by F_1-ATPase. Nature 427, 465–468.

Liu, D.S., Astumian, R.D., Tsong, T.Y., 1990. Activation of the Na^+-pumping and the K^+-pumping modes of Na,K-ATPase by oscillating electric field. J. Biol. Chem. 265, 7260–7267.

Makhnovskii, Y.A., Rozenbaum, V.M., Yang, D.Y., Lin, S.H., Tsong, T.Y., 2004. Flashing ratchet model with high efficiency. Phys. Rev. E 69, 021102.

Markin, V.S., Liu, D.S., Gimsa, J., Strobel, R., Rosenberg, M.D., Tsong, T.Y., 1992. Ion channel-enzyme in an oscillating electric field. J. Membrane Biol. 16, 137–145.

Markin, V.S., Tsong, T.Y., 1991. Electroconformational coupling for ion transport in an oscillating electric field: rectification versus active pumping. Bioelectrochem. Bioenerg. 26, 251–276.

Markin, V.S., Tsong, T.Y., 1991. Frequency and concentration windows for the electric activation of a membrane active transport system. Biophys. J. 29, 982–987.

Markin, V.S., Tsong, T.Y., 1991. Reversible mechanosensitive ion pumping as a part of mechanoelectric transduction. Biophys. J. 59, 1317–1324.

Markin, V.S., Tsong, T.Y., 1993. Thermodynamics of membrane transport in oscillating fields, Modern Aspect of Electrochemistry, vol. 24. Plenum Press, NY 39–122.

Markin, V.S., Tsong, T.Y., Astumian, R.D., Robertson, M., 1990. Energy transduction between a concentration gradient and an alternating electric field. J. Chem. Phys. 93, 5062–5066.

Nicholls, J.G., Martin, A.R., Wallace, B.G., 1992. From Neuron to Brain. Sinauer Associates, Inc., Sunderland, MA.

Rozenbaum, V.M., Korochkova, T.Y., Yang, D.Y., Lin, S.H., Tsong, T.Y., 2005. Two approaches toward a high-efficiency flashing ratchet. Phys. Rev. E 71, 041102.

Rozenbaum, V.M., Yang, D.Y., Lin, S.H., Tsong, T.Y., 2004. Catalytic wheel as a Brownian motor. J. Phys. Chem. B 108, 15880–15889.

Serpersu, E.H., Tsong, T.Y., 1983. Stimulation of Rb+ pumping activity of Na,K-ATPase in human erythrocytes with an external electric field. J. Membrane Biol. 74, 191–201.

Serpersu, E.H., Tsong, T.Y., 1984. Activation of electrogenic Rb+ transport of Na,K-ATPase by an electric field. J. Biol. Chem. 259, 7155–7162.

Teissie, J., Knox, B.E., Tsong, T.Y., Wehrle, J., 1981. Synthesis of adenosine triphosphate in respiration inhibited submitochondrial particles induced by microsecond electric pulses. Proc. Natl. Acad. Sci. U.S.A. 78, 7473–7477.

Tinoco Jr., I., Sauer, K., Wang, J.C., Puglisi, J.D., 2002. Physical Chemistry, Principles and Applications in Biological Sciences, fourth ed. Prentice Hall, Upper Saddle River, NJ.

Tsong, T.Y., 1990. Electrical modulation of membrane proteins: enforced conformational oscillations and biological energy and signal transductions. Annu. Rev. Biophys. Biophys. Chem. 19, 83–106.

Tsong, T.Y., Astumian, R.D., 1986. Absorption and conversion of electric field energy by membrane bound ATPases. Bioelectrochem. Bioenerg. 15, 457–476.

Tsong, T.Y., Astumian, R.D., 1987. Electroconformational coupling and membrane protein function. Prog. Biophys. Mol. Biol. 50, 1–45.

T.Y. Tsong, C.H. Chang, (2003). Catalytic wheel, Brownian motor, and biological energy transduction. AAPPS Bull. 13(No 2), 12–18, http://www.aapps.org/archive/bulletin/vol13/vol13.html.

Tsong, T.Y., Chang, C.H., 2005. Enzyme as catalytic wheel powered by a Markovian engine: conformational coupling and barrier surfing models. Physica A 350, 108–121.

Tsong, T.Y., Hearn, R.P., Wrathall, D., Sturtevant, J.M., 1970. A calorimetric study of thermally induced conformational transitions of ribonuclease A and certain of its derivatives. Biochemistry 9, 2666–2677.

Tsong, T.Y., Su, Z.D., 1999. Does proline isomerization shape the folding funnel of the wild type and mutant staphylococcal nuclease? Biol. Phys. APS Third Int. Symp. 37–53.

Vale, V.D., Funatsu, T., Pierce, D.W., Romberg, L., Harada, Y., Yanagida, T., 1996. Direct observation of single kinesin molecules moving along microtubules. Nature 4, 451–453.

Wang, H., Oster, G., 1998. Nature 396, 279–282.

Weaver, J.C., Vaughan, T.E., Martin, G.T., 1999. Biological effects due to weak electric and magnetic fields: the temperature variation threshold. Biophys. J. 76 (6), 3026–3030.

Xie, T.D., Chen, Y.D., Marszalek, P., Tsong, T.Y., 1997. Noise-induced flux in biochemical cycle: further study of electric activation of Na,K-pumps. Biophys. J. 72, 2496–2502.

Xie, X.S., Lu, H.P., 1998. Single-molecule enzymology. J. Biol. Chem. 274, 15967–15970.

Xie, T.D., Marszalek, P., Chen, Y.D., Tsong, T.Y., 1994. Recognition and processing of randomly fluctuating electric signals by Na,K-ATPase. Biophys. J. 66, 1251–1257.

Yasuda, R., Noji, H., Kinosita Jr., K., Yoshida, M., 1998. F_1-ATPase is a highly efficient molecular motor that rotates with discrete 120° steps. Cell 93, 1117–1124.

Yasuda, R., Noji, H., Yoshida, M., Kinosita Jr., K., Itoh, H., 2001. Resolution of distinct rotational substeps by sumillisecond kinetic analysis of F_1-ATPase. Nature 410, 898–904.